Homogenisation of reflected solar fluxes in the Climate Monitoring SAF

S. Dewitte[1], N. Clerbaux, B. Nicula

Royal Meteorological Institute of Belgium, Department of Observations, Section Remote Sensing from Space, Ringlaan 3, B-1180 Brussels, Belgium.
Vrije Universiteit Brussel (VUB), Faculty of Applied Sciences, Department of electronics, Pleinlaan 2, B-1050 Brussels, Belgium.

Abstract

One of the goals of the Climate Monitoring Satellite Application Facility (CM-SAF) is to provide consistent cloud and radiation parameters in high spatial resolution for an area that covers at least Europe and part of the North Atlantic Ocean. Daily means, monthly means and monthly mean diurnal cycles are to be provided. At the Top Of the Atmosphere (TOA) the three radiative flux components of incoming solar radiation, reflected solar radiation and emitted thermal radiation will be given.

In this paper the method used within the CM SAF facility for the homogenisation of the TOA reflected solar fluxes is described, and results using currently available input data are shown.

As input data reflected solar fluxes from METEOSAT and CERES (Clouds and the Earths Radiant Energy System) are used. Once MSG (METEOSAT Second Generation) fluxes will become available, they will replace the METEOSAT fluxes.

The homogenisation consists of the detection and the removal of the systematic dependencies of the flux estimates on scene type and viewing angles. For a given scene type and solar zenith angle, the mean of the CERES measurements over all viewing zenith angles and relative azimuths is used as the reference for the homogenisation.

1 Introduction

The radiative flux F is defined as the integral over the upper hemisphere of the vertical components of all the radiances upwelling at the top of the atmosphere above a given region on earth. From a broadband satellite measurement the radiance L in one single direction is known. An estimate $\hat{F}$ of the true flux F can be derived from the measured radiance L using a *model* of the angular distribution of the upwelling radiance. For the reflected solar radiation one usually puts (*Wielicki et al*(1996), *Dewitte et al*(2000)):

$$\hat{F} = \frac{\pi L}{R(\text{scene}, \theta_s, \theta, \phi)} \tag{1}$$

R is a model of the bidirectional reflectance as a function of the scene type, the solar zenith angle θ_s, the viewing zenith angle θ and the relative azimuth angle ϕ. As the (unknown) true bidirectional reflectance is different from the model one, some residual error $F - \hat{F}$ will exist. It can be expected that this error is a function of the same variables as the bidirectional reflectance.

$$F - \hat{F} = f(\text{scene}, \theta_s, \theta, \phi) \tag{2}$$

In this paper we will estimate the mean values $\overline{F - \hat{F}}$ for the METEOSAT and CERES derived reflected solar fluxes. The scene types will be grouped in three surface scene type classes - ocean, land and desert - and two

[1]Email: Steven.Dewitte@oma.be

cloudiness classes - a low amount of cloudiness indicated by an albedo < 0.4, and a high amount of cloudiness indicated by an albedo ≥ 0.4. The viewing angles θ_s, θ will be grouped in intervals of 15 degrees and ϕ will be grouped in intervals of 30 degrees.

2 METEOSAT and CERES viewing conditions

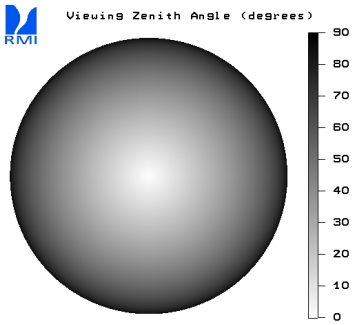

Figure 1: METEOSAT viewing zenith angles.

As METEOSAT is a geostationary satellite, it observes a given region of the earth with a fixed viewing zenith angle. For a given period of the year, the relative azimuth varies with the hour of the day as the sun (apparently) rotates around the earth. Figure 1 shows the METEOSAT viewing zenith angle image.

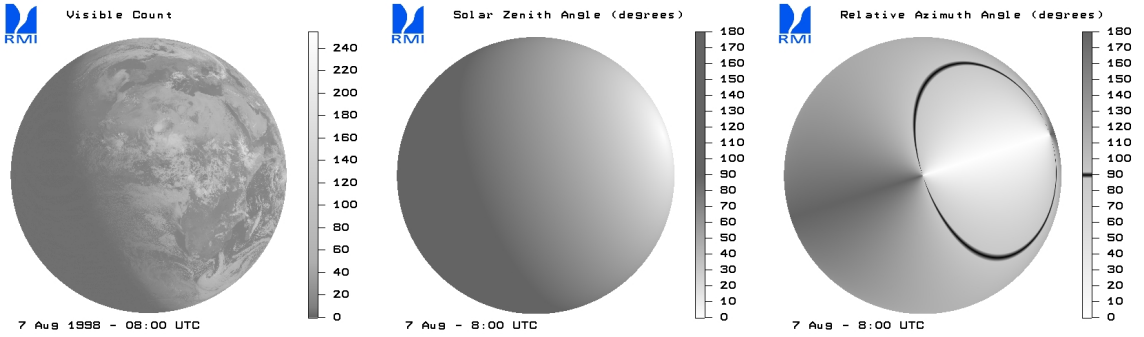

Figure 2: Left: Morning METEOSAT visible image. Mid: Corresponding solar zenith angles. Right: Corresponding relative azimuth angles.

Figure 2 shows a typical morning visible image, together with the corresponding solar zenith angle and relative azimuth angle image. The relative azimuth angle image shows two discontinuities. The central discontinuity corresponds to the METEOSAT nadir, where the viewing zenith angle is zero. The eastern discontinuity near the limb corresponds to the position of the sun, where the solar zenith angle is zero. During the day the sun moves from east to west relative to the earth, and so does the point of 0° solar zenith angle, and the second dicontinuity of the relative azimuth.

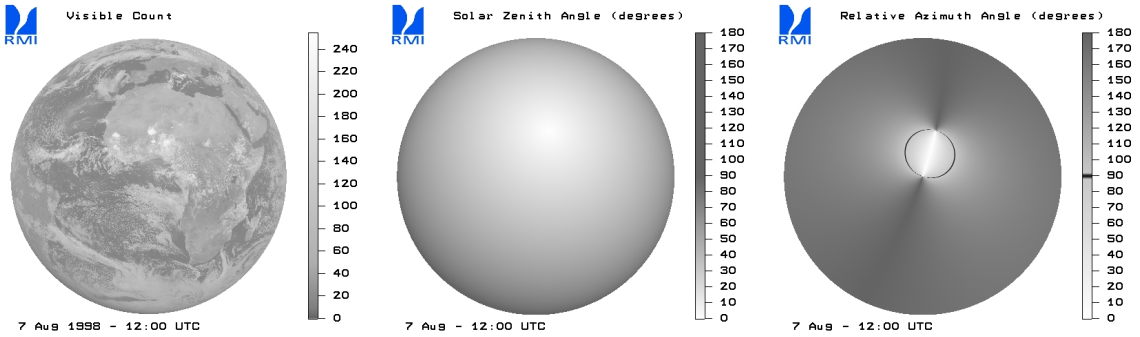

Figure 3: Left: Noon METEOSAT visible image. Mid: Corresponding solar zenith angles. Right: Corresponding relative azimuth angles.

Figure 3 shows a typical noon visible image, together with the corresponding solar zenith angle and relative azimuth angle image. The position of the sun is now close to the center of the images.

Only points on earth contained within the black arc on the relative azimuth images like the ones of figures 2 and 2 are observed by METEOSAT in forward scattering direction. Most points are observed during all or most times of the day in backward scattering direction.

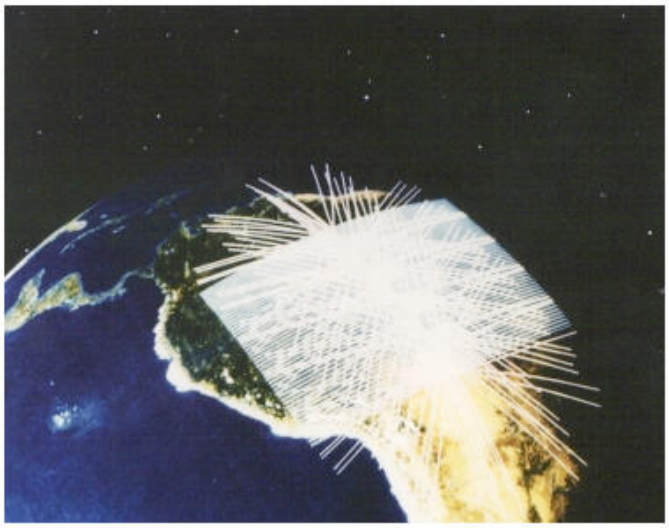

Figure 4: CERES scanning. Scan patterns on earth for fixed and rotating scan plane.

CERES flies around the earth on a satellite in a low earth orbit. The CERES radiometer scans the earth in a plane which can be rotated relative to the satellite flight direction, see figure 4. . The two most common CERES instrument modes are cross-track scanning - where the scan plane is kept fixed perpendicular to the flight direction - and rotating azimuth plane scanning (RAPS) - where the scan plane rotates at constant speed relative to the flight direction. In this paper we use RAPS data from the CERES instrument on the Tropical Rainfall Measuring Mission (TRMM) satellite colocated with METEOSAT 7 data. This data covers one out of three days during June, July and August 1998.

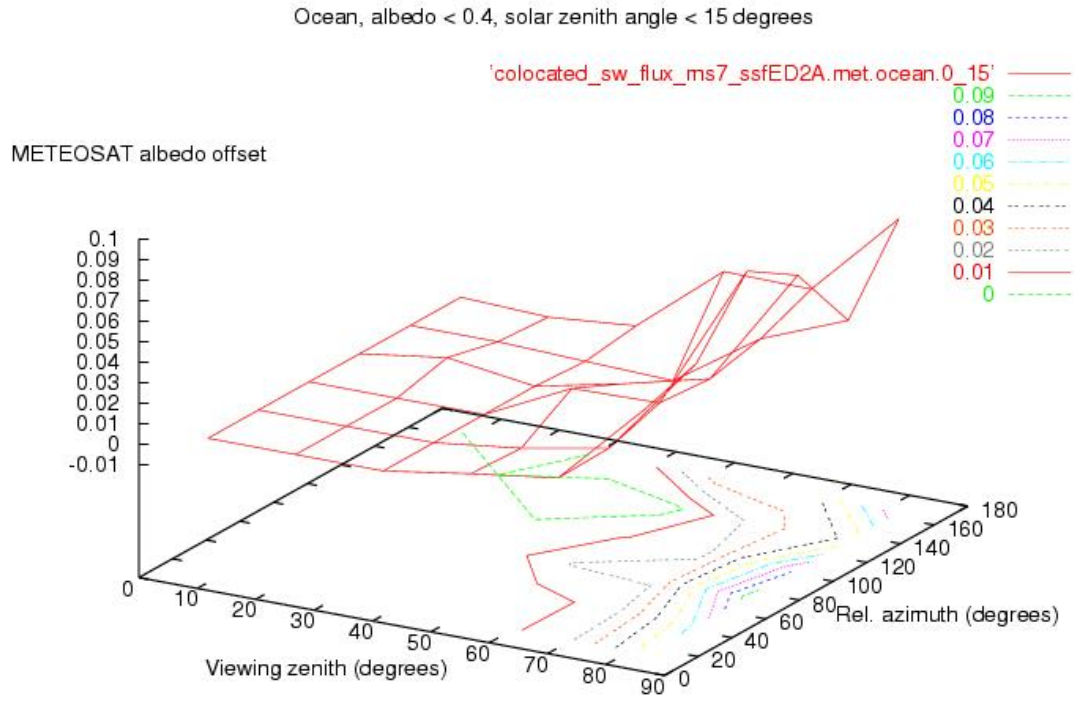

Figure 5: Offset of METEOSAT relative to mean CERES as a function of the viewing zenith and relative azimuth angle. Surface scene type: ocean. Solar zenith angles are between 0 and 15 degrees.

3 METEOSAT homogenisation

For any given combination of a surface scene type (ocean, land or desert), cloudiness class (albedo < 0.4 or ≥ 0.4), and 15° solar zenith angle interval, we calculate the mean offset of the METEOSAT flux relative to the colocated CERES flux as a function of the METEOSAT viewing angles θ, ϕ. As we use CERES fluxes in RAPS mode, there is a good random sampling of all viewing zenith and relative azimuth angles by CERES. Therefore we associate the mean CERES flux with the true flux. Figure 5 shows the METEOSAT offset - expressed in function of the albedo - obtained for the ocean surface type, low cloudiness (albedo < 0.4) and high sun ($0 <= \theta_s < 15°$). For this case there is a systematic increase of the METEOSAT albedo offset with viewing zenith angle. The minimum value for the albedo offset is 0 %, the maximum value is 9 %. In tables 1 and 2 the minimum and maximum albedo offsets are given for all combinations of surface scene type, solar zenith angle interval and cloudiness class (table 1 = low cloudiness, table 2 = high cloudiness). The case corresponding to figure 5 is indicated in boldface in table 2.

solar zenith angle	$0-15°$	$15-30°$	$30-45°$	$45-60°$	$60-75°$	$75-90°$
ocean	**−0.00/0.09**	−0.00/0.02	−0.02/0.03	−0.01/0.05	−0.02/0.07	−0.11/0.04
land	−0.01/0.04	−0.02/0.03	−0.02/0.04	−0.03/0.05	−0.02/0.04	−0.05/0.07
desert	−0.01/0.03	−0.01/0.03	−0.02/0.02	−0.01/0.03	−0.02/0.06	0.00/0.05

Table 1: Min/max albedo offsets for METEOSAT fluxes relative to mean CERES, albedo < 0.4

The METEOSAT albedos are homogenised by subtracting the offset relative to the mean CERES albedos.

solar zenith angle	$0-15°$	$15-30°$	$30-45°$	$45-60°$	$60-75°$	$75-90°$
ocean	$-0.01/0.04$	$-0.01/0.05$	$-0.01/0.05$	$-0.03/0.08$	$-0.02/0.15$	$-0.08/0.18$
land	$-0.01/0.08$	$-0.01/0.07$	$-0.02/0.04$	$-0.04/0.08$	$-0.10/0.13$	$0.00/0.27$
desert	$-0.01/0.00$	$-0.01/0.05$	$0.00/0.04$	$-0.03/0.05$	$-0.01/0.16$	$0.00/0.00$

Table 2: Min/max albedo offsets for METEOSAT fluxes relative to mean CERES, albedo ≥ 0.4

4 CERES homogenisation

Once the METEOSAT albedos (or fluxes) are homogenised, they can be used as a reference for the homogenisation of CERES. The offsets of the CERES albedos relative to the homogenised METEOSAT albedos - and hence relative to the mean CERES - are derived analoguously as in the previous section. For any given combination of a surface scene type (ocean, land or desert), cloudiness class (albedo < 0.4 or ≥ 0.4), and $15°$ solar zenith angle interval, we calculate the mean offset of the CERES albedo relative to the colocated homogenised METEOSAT albedo as a function of the CERES viewing angles θ, ϕ. The minimum and maximum CERES albedo offsets relative to the homogenised METEOSAT are given in tables 3 and 4 (table 3 = low cloudiness, table 4 = high cloudiness).

solar zenith angle	$0-15°$	$15-30°$	$30-45°$	$45-60°$	$60-75°$	$75-90°$
ocean	$-0.01/0.01$	$-0.00/0.01$	$-0.01/0.01$	$-0.01/0.01$	$-0.02/0.01$	$-0.03/0.03$
land	$-0.01/0.00$	$-0.01/0.01$	$-0.01/0.00$	$-0.00/0.04$	$-0.03/0.05$	$-0.09/0.04$
desert	$-0.00/0.01$	$-0.01/0.00$	$-0.01/0.00$	$-0.03/0.02$	$-0.03/0.04$	$0.00/0.00$

Table 3: Min/max albedo offsets for the CERES flux for particular viewing angles relative to the mean of the CERES fluxes over all viewing angles, albedo < 0.4

solar zenith angle	$0-15°$	$15-30°$	$30-45°$	$45-60°$	$60-75°$	$75-90°$
ocean	$-0.05/0.06$	$-0.05/0.02$	$-0.01/0.03$	$-0.03/0.01$	$-0.04/0.01$	$-0.06/0.03$
land	$-0.02/0.02$	$-0.02/0.02$	$-0.03/0.02$	$-0.03/0.04$	$-0.04/0.05$	$-0.04/0.05$
desert	$-0.02/0.02$	$-0.05/0.02$	$-0.00/0.04$	$-0.03/0.04$	$-0.03/0.02$	$0.00/0.00$

Table 4: Min/max albedo offsets for the CERES flux for particular viewing angles relative to the mean of the CERES fluxes over all viewing angles, albedo ≥ 0.4

The CERES albedos are homogenised by subtracting the offset relative to the homogenised METEOSAT albedos.

5 Discussion of results

Tables 1,2,3,4 give the maximum absolute measured systematic errors of the METEOSAT and CERES derived albedos as a function of scene type and solar zenith angle. These errors are defined relative to the mean CERES flux - where the mean is defined as the mean over all CERES viewing angles θ, ϕ.

In general the maximum absolute measured systematic errors increase with increasing solar zenith angle (going from left to right in tables 1,2,3,4). However, as for a higher solar zenith angle the flux level decreases as $\cos(\theta_s)$, the impact on the absolute flux errors of the high sun cases is mitigated.

For low cloudiness cases, the CERES albedo errors (table 3) are mostly lower then the METEOSAT albedo errors (table 1), particularly for the high sun cases (left part tables). For low cloudiness and high sun, CERES reaches the accuracy of +/- 1 %.

In general, it can not be garantueed that the systematic errors are within +/-5 %, or even +/- 10 %. At these levels of error, the proposed homogenisation is mandatory prior to the merging of both datasets.

References

[1] Wielicki, B. and Barkstrom, B.R. and Harrison, E.F. and Lee, R.B. and Smith, G.L. and Cooper, J.E., 1996. Clouds and the Earth's Radiant Energy System (CERES): An Earth Observing System Experiment. *Bulletin of the American Meteorological Society*, **77**:853–868.

[2] Dewitte, S. and Clerbaux, N. and Gonzalez, L. and Hermans, A. and Ipe, A. and Joukoff, A. and Sadowski, G. 2000. Generation of GERB unfiltered radiances and fluxes. *Proceedings of the 2000 EUMETSAT Meteorological Satellite Data Users' Conference*, 72–78.

Acknowledgment

All METEOSAT images used for this study were obtaind from the METEOSAT Archive and Retrieval Facility at EUMETSAT. All CERES products used for this study were obtained from the NASA Langley Distributed Active Archive Center. Figure 4 was obtained from the CERES web site, http://asd-www.larc.nasa.gov/ceres/ASDceres.html. This study was performed as part of the development of the Climate Monitoring Satellite Application Facility for EUMETSAT. This study was supported by the Belgian Science Policy Office (DWTC/SSTC) through the PRODEX program.